

Investigation of the structural and magnetic properties of TeO₂- based glasses modified by rare earth (La₂O₃, Gd₂O₃, Er₂O₃, and Ho₂O₃) using as an optical isolator

A. M. Al-Syadi^{a,b}, M. Alfarh^{c,d}, H. Algarni^{c,d}, M. S. Alqahtani^e, M. Reben^f,
H. Afifi^g, El Sayed Yousef^{c,d,h,*}

^aDepartment of Physics, Faculty of Science and Arts, Najran University, Saudi Arabia.

^bDepartment of Physics, Faculty of Education, Ibb University, Yemen.

^cPhysics Dep., Faculty of Science, King Khalid University, P. O. Box 9004, Abha, Saudi Arabia

^dResearch Center for Advanced Materials Science (RCAMS), King Khalid University, Postcode: 9004, Zip code: 61413, Abha, Saudi Arabia

^eDepartment of Radiological Sciences, College of Applied Medical Sciences, King Khalid University, Abha 61421, Saudi Arabia.

^fFaculty of Materials Science and Ceramics, AGH – University of Science and Technology, al. Mickiewicza 30, 30-059 Cracow, Poland

^gUltrasonic Laboratory, National Institute for Standards, Tersa Street El-haram, El-Giza, P.O. Box 136, Code N 12211, Egypt

^hPhysics department, Faculty of Science, Al Azhar University, Assiut Branch, Egypt

Tellurite glasses with a composition of 76TeO₂-10ZnO-9PbO-1.0PbF₂-3.0Nb₂O₅- 1.0 x in mol% modified with different rare earth oxides (where x= La₂O₃, Gd₂O₃, Er₂O₃, and Ho₂O₃). The magnetic properties such as; Faraday effect and the Verdet constant at the intensity of the laser beam ($\lambda = 632$ nm) of the present glasses were measured. The glass contains La₂O₃ has the highest value of Verdet constant, ($V = 0.102$ min/G.cm) otherwise the sample has Ho₂O₃ has the lowest value of Verdet constant ($V = 0.069$ min/G.cm). It means that V- value strongly depends on the polarizability of rare earth. An optical isolator is a unidirectional light gate, which can prevent the back reflection of light into lasers or optical amplifiers and reduce signal instability and noise. Finally, the structure of prepared glasses was investigated by Raman spectra.

(Received June 14, 2021; Accepted September 17, 2021)

Keywords: Rare earth, Structural, Magnetic properties, Optical isolator, Faraday effect

1. Introduction

Optical technologies and optoelectronic devices are made from a variety of materials, including glasses. This is related to the optical capabilities of the glasses, which may absorb certain wavelengths and operate as optical filters, as well as be sources of radiation at various frequencies and emit coherent laser light under specified circumstances [1]. Special glasses are used in fiber optics and optoelectronics for telecommunications because they can transmit light over long distances and modify the frequency of incoming radiation [1, 2].

Tellurite-based glasses provide several advantages, including low phonon energy, a high refractive index, a high dielectric constant, superior corrosion resistance, excellent thermal and chemical stability, and a low melting point [3]. New TeO₂-based glasses that mix rare earth with are particularly attractive optical amplifier materials in a broad range for wavelength division multiplexing (WDM) network systems have recently been developed [3, 4]. Rare earth oxides with unique electrical characteristics have the potential to be used as catalysts, high dielectric constant gate oxides, laser dopants, and magneto-optic memory materials [5]. Laser rods and disk

* Corresponding author: omn_yousef2000@yahoo.com

amplifiers, optical sensors, solar cells, optical communication, white light-emitting diodes, and optical data storage systems all use rare earth-doped glass [6, 7].

Due to their unusual electrochemical, magnetic, catalytic, and luminous capabilities, rare-earth (lanthanide) compounds have recently received a lot of interest [8, 9, 10]. The optical characteristics of linear and non-linear glasses doped with transition metals and rare earth, particularly lanthanides, have enabled improvements in the design and application of novel glassy matrices for widely recognized optoelectronics and photonics in recent years. Optical phenomena in glasses are not only helpful, but they also provide information about their internal structure, including the characteristics of optical spectra in the ultraviolet, visible, and infrared spectrum [1, 11]. Faraday rotation, or magneto-optical rotation of light polarization, is significant for a variety of applications, including optical isolators and optical diodes inside laser resonators [12]. The Verdet constant [13] determines the intensity of the Faraday Effect in a material. The Verdet constant's magnitude is determined by the gain medium host, the dopant and its concentration, the oscillation wavelength, and the temperature [12]. In the diamagnetic glass, however, the Faraday rotation effect may be enhanced by doping strongly polarized diamagnetic ions or creating surface Plasmon Resonance (SPR) effects [14].

In rare-earth iron garnets, bismuth and lead are known to cause substantial magneto-optical effects. This has resulted in several basic studies as well as the creation of technological applications [15,16,17]. Lead is usually utilized in glasses to increase magnetic or magneto-optical activity due to its great diamagnetic susceptibility and high polarizability. These characteristics imply that a large value of the Verdet constant [18- 20] might be seen.

The TeO₂-based glasses (76TeO₂- 10ZnO- 9PbO-1.0PbF₂- 3.0Nb₂O₅-1.0x in mol %) doped with various rare earth oxides (where x= La₂O₃, Gd₂O₃, Er₂O₃, and Ho₂O₃) were produced utilizing the melt-quenching approach, which was less cost-effective and moment. The Faraday effect was explored, and Raman spectroscopy was used to examine the structure of these glasses.

2. Experimental Work

Using the standard quench-melting approach, glass systems with a composition of 76TeO₂-10ZnO-9.0PbO-1.0PbF₂- 3.0Nb₂O₅-1.0x mol % with various rare earth oxides (where x= La₂O₃, Gd₂O₃, Er₂O₃, and Ho₂O₃) were created. The raw ingredients were pulverized and placed in a platinum crucible, which was heated in a melting furnace to 920°C for 45 minutes, with the melt being stirred occasionally. A graphite mold was used to cast the very viscous melt. The quenched samples were annealed at 340°C for 2 hours before being cooled to room temperature within the furnace. Table 1 shows the chemical composition of the analyzed tellurite glasses.

The schematic description of the setup used to obtain the Verdet constants for various glasses and Raman spectra were shown in Ref. [21].

Table 1. The Verdet constant (*V*) and refractive index (*n*) at $\lambda = 632 \text{ nm}$ of the TeO₂-based glasses (76TeO₂-10ZnO-9PbO-1.0PbF₂-3.0Nb₂O₅-1.0La₂O₃ mol%) doped with different rare earth oxides.

Sample code	Composition in mol%	Verdet constant V(min/G.cm)
Sample 1	76TeO ₂ -10ZnO-9PbO-1.0PbF ₂ -3.0Nb ₂ O ₅ -1.0La ₂ O ₃	0.102
Sample 2	76TeO ₂ -10ZnO-9PbO-1.0PbF ₂ -3.0Nb ₂ O ₅ -1.0La ₂ O ₃ - doped 1.0 Gd ₂ O ₃	0.0917
Sample 3	76TeO ₂ -10ZnO-9PbO-1.0PbF ₂ -3.0Nb ₂ O ₅ -1.0La ₂ O ₃ - doped 1.0 Er ₂ O ₃	0.095
Sample 4	76TeO ₂ -10ZnO-9PbO-1.0PbF ₂ -3.0Nb ₂ O ₅ -1.0La ₂ O ₃ - doped 1.0 Ho ₂ O ₃	0.069

3. Results and discussion

The Zeeman splitting of atomic energy levels causes the magneto-optical rotation of light's polarization [13]. The left and right circularly polarised components of a linearly polarised laser

beam would have different refractive indices and so travel at different rates for the desired direction of propagation through a magneto-optical material to which a magnetic field is applied. When a result, as a linearly polarised laser beam propagates through such a material, the plane of polarisation of the incoming laser beam rotates [12]. The rotating angle of glass is linked to the magnetic field B , the Verdet constant (V), and the glass length L in the following equation [15], according to Faraday rotation theory:

$$\theta = VLB \quad (1)$$

To verify the self-constructed setup, the relation between the current and current-produced-magnetic field expressed in Eq (2) [15] was studied.

$$B = \frac{\mu_0 NI}{L_s} \quad (2)$$

where μ_0 is a constant of $1.26 \times 10^{-6} \text{ Hm}^{-1}$, N is the turn numbers of coil surround the solenoids, I is the current go through the solenoids, L_s is the length of solenoids. The current and magnetic field presented a linear relationship, as shown in Fig. 1, indicating the stability of the solenoid.

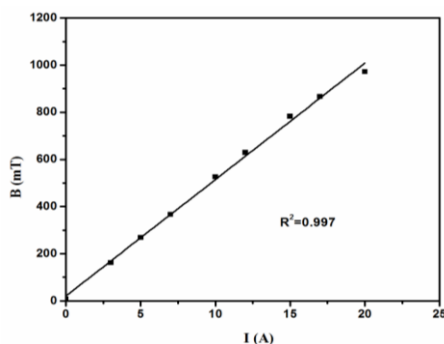


Fig. 1. Relation between the current (I) and magnetic field (B).

Fig. 2 (a-d) shows the θ of samples with fixed length L as a function of magnetic field B , it can be that all samples appear the θ increased with the increase of B . The slope indicates to Verdet constant (V) that is calculated by (slope = VL). The values of the Verdet constant (at $\lambda=632 \text{ nm}$) for samples are listed in Table 1. These values of the Verdet constant are in good agreement with previously available reports [1,15], but these glasses presented higher results than those reported in the literature [21]. The Faraday Effect experiments were able to observe the phenomena of light distorting its plane of polarization under the influence of a longitudinal magnetic field in all of the studied glasses. Figure 4 shows the maximum values of Verdet constants derived on this basis. In comparison to the glass samples containing La_2O_3 , Gd_2O_3 , Er_2O_3 , and Ho_2O_3 , the glass sample ($76\text{TeO}_2\text{-}10\text{ZnO-}9\text{PbO-}1.0\text{PbF}_2\text{-}3.0\text{Nb}_2\text{O}_5\text{-}1.0\text{La}_2\text{O}_3$ in mol%) demonstrated the highest value of V . This could be due to the presence of a rare earth modifier in the matrix of tellurite glasses. The larger value of the observed magnetic susceptibility [18] is most likely the factor that influences such a difference in the V of the studied glasses. Because they have a higher value of Verdet constant, the result obtained the prepared glasses contains rare earth especially La_2O_3 could suggest that are potentially better materials for magneto-optical systems.

In comparison to the same glassy matrix including La_2O_3 , Gd_2O_3 , Er_2O_3 , and Ho_2O_3 , the sample doped with Er_2O_3 exhibits high V values, as seen in Fig. 3. In all examined glass compositions, doping the glasses with paramagnetic erbium ions resulted in the expected increase in the angle of rotation of the light polarization plane under the influence of the magnetic field, which is consistent with the previously observed increase in magnetic susceptibility.

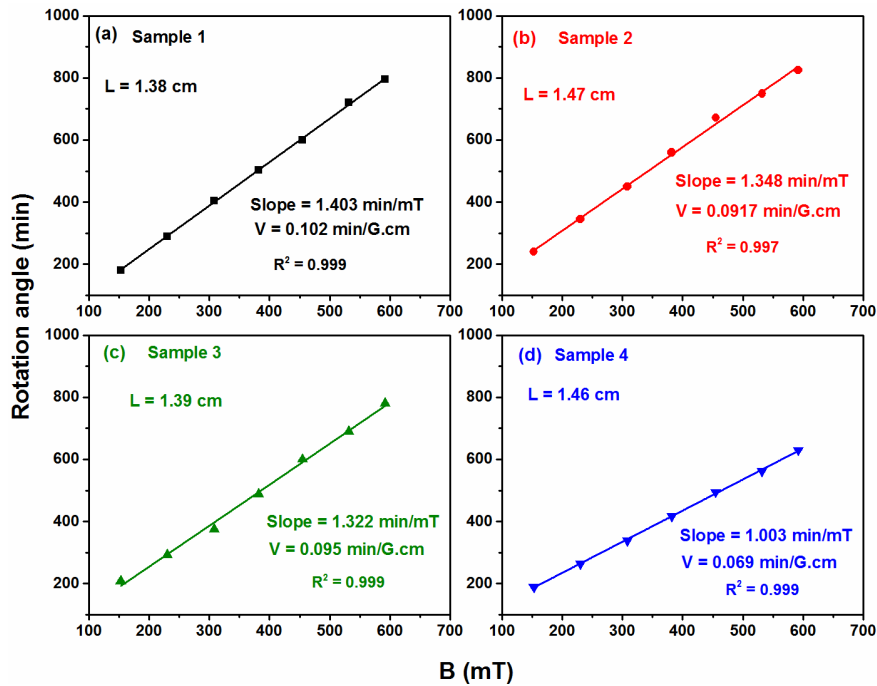


Fig. 2. Relation between magnetic field B and Faraday rotation angle θ for the TeO_2 -based glasses (76TeO_2 - 10ZnO - 9PbO - 1.0PbF_2 - $3.0\text{Nb}_2\text{O}_5$ - $1.0\text{La}_2\text{O}_3$ mol%) doped with different rare earth oxides: (a) without doping; (b) doped with Gd_2O_3 ; (c) Er_2O_3 and (d) Ho_2O_3 .

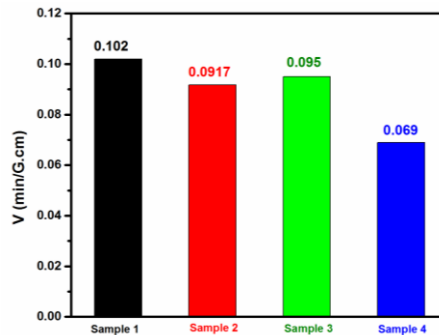


Fig. 3. Verdet constants of the TeO_2 -based glasses (76TeO_2 - 10ZnO - 9PbO - 1.0PbF_2 - $3.0\text{Nb}_2\text{O}_5$ - $1.0\text{La}_2\text{O}_3$ mol%) doped with different rare earth oxides.

The Raman spectrum is a useful tool for investigating the structure of glass materials. The Raman spectra of the undoped 76TeO_2 - 10ZnO - 9PbO - 1.0PbF_2 - $3.0\text{Nb}_2\text{O}_5$ - $1.0\text{La}_2\text{O}_3$ glass and doped with several rare earth oxides (La_2O_3 , Gd_2O_3 , Er_2O_3 , and Ho_2O_3) are shown in Fig. 5 (a-d), which were deconvoluted using Gaussian fitting. The Raman spectra of the undoped 76TeO_2 - 10ZnO - 9PbO - 1.0PbF_2 - $3.0\text{Nb}_2\text{O}_5$ - $1.0\text{La}_2\text{O}_3$ glass are shown in Fig. 4a (Sample 1). The disordered features in this glass are primarily responsible for a large scattering peak. At about 653 , 653 , 721 , and 768 cm^{-1} , the spectra can be further divided into four symmetrical Gaussian peaks. Stretching vibrations of the Te-O bond in TeO_4 trigonal bipyramidal structural units are responsible for the peaks about 653 cm^{-1} [22].

Stretching vibrations of $\text{TeO}_3/\text{TeO}_{3+1}$ units are responsible for the peak around 721 cm^{-1} while bending vibrations of Te-O bond and Te=O double bonds in $[\text{TeO}_3]$ and distorted $[\text{TeO}_{3+1}]$ trigonal pyramidal [24] are responsible for the peak at 768 cm^{-1} . The Raman spectra of 76TeO_2 - 10ZnO - 9PbO - 1.0PbF_2 - $3.0\text{Nb}_2\text{O}_5$ glasses with Gd_2O_3 in place of La_2O_3 are shown in Fig. 4b

(Sample 2). At 648, 648, 745, and 878 cm^{-1} , the spectra can be further divided into four symmetrical Gaussian peaks. Anti-symmetrical stretching of the continuous network formed of TeO_4 tbps is responsible for the peaks about 648 cm^{-1} [25]. Stretching vibrations of TeO_4 tbp [23] are thought to be responsible for the peak at 745 cm^{-1} while stretching vibrations of Nb–O bonds in NbO 6 octohedra are responsible for the peak around 878 cm^{-1} . The Raman spectra of the glass $76\text{TeO}_2\text{-}10\text{ZnO-}9\text{PbO-}1.0\text{PbF}_2\text{-}3.0\text{Nb}_2\text{O}_5$ glasses La_2O_3 changed with Er_2O_3 is shown in Fig. 5c (Sample 3). A broad scattering peak at about 406, 502, 565, 694, and 800 cm^{-1} was deconvoluted using Gaussian fitting to five peaks.

The symmetrical stretching or bending vibrations of Te–O–Te links, which are produced by corner-sharing of (TeO_4) , (TeO_{3+1}) polyhedral, and TeO_3 units, are responsible for the peaks about 406 cm^{-1} [27]. The peak around 502 cm^{-1} could be due to the axial symmetrical stretching modes of TeO_4 tetrahedra $(\text{Te}_{\text{ax}}\text{-O})_s$ [27]. Anti symmetrical stretching of the continuous TeO_4 tbps network is responsible for the peak of about 565 cm^{-1} [25]. The $(\text{Te}_{\text{eq}}\text{O})_s$ and $(\text{Te}_{\text{eq}}\text{O})_a$ s vibration modes of TeO_{3+1} polyhedra or TeO_3 trigonal bipyramids units are ascribed to the band at 694 cm^{-1} , however, the peak at 800 cm^{-1} is assigned to stretching vibrations of Nb–O bonds in NbO_6 octohedra [26, 27].

Figure 4d depicts the Raman spectrum of an undoped $76\text{TeO}_2\text{-}10\text{ZnO-}9\text{PbO-}1.0\text{PbF}_2\text{-}3.0\text{Nb}_2\text{O}_5$ glass treated with Ho_2O_3 (Sample 4). This glass's disordered features are responsible for the wide scattering peak. At about 208, 363, 506, and 653 cm^{-1} , the spectra may be broken further into four symmetrical Gaussian peaks. The vibration of Nb–O in NbO_6 octahedra is responsible for the peak of about 208 cm^{-1} . The axial bending vibration mode (OaxTe-Oax) at corner sharing sites [25] can be attributed to the peak of about 363 cm^{-1} . The axial symmetrical stretching modes of $(\text{Te}_{\text{ax}}\text{-O})_s$ of TeO_4 tetrahedra may be responsible for the peak of about 506 cm^{-1} . Finally, stretching vibrations of the TeO bond in TeO_4 trigonal bipyramidal structural units can be attributed to the peaks about 653 cm^{-1} [22].

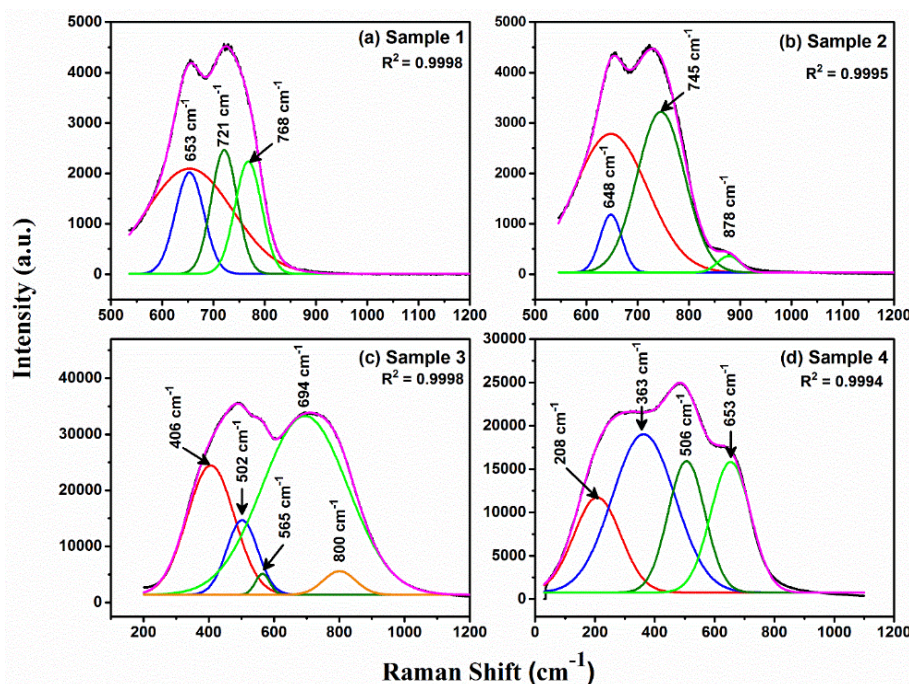


Fig. 4. Raman spectra of the TeO_2 -based glasses ($76\text{TeO}_2\text{-}10\text{ZnO-}9\text{PbO-}1.0\text{PbF}_2\text{-}3.0\text{Nb}_2\text{O}_5\text{-}1.0\text{La}_2\text{O}_3$ mol%) doped with different rare earth oxides: (a) without doping; (b) doped with Gd_2O_3 ; (c) Er_2O_3 and (d) Ho_2O_3 .

4. Conclusion

The present glasses matrix $\text{TeO}_2\text{-ZnO- PbO-PbF}_2\text{- Nb}_2\text{O}_5$ includes different rare earth such as La_2O_3 , Gd_2O_3 , Er_2O_3 , Ho_2O_3 can be used as an optical isolator. The glasses contain La_2O_3 have the highest value of the Verdet constant. The value of the Verdet constant of prepared glasses is in the range from 0.102 to 0.69 min/G.cm. The Stretching vibrations of $\text{TeO}_3/\text{TeO}_{3+1}$ units are confirmed to be the peak at 721 cm^{-1} . The bending vibrations of the Te-O bond and Te=O double bonds appeared at the peak 768 cm^{-1} .

Acknowledgments

The authors extend their appreciation to the Deanship of Scientific Research at King Khalid University (KKU) for funding this research project Number (R.G. P2/63/40). Also, the authors extend their appreciation to the Scientific Research Deanship at King Khalid University and the Ministry of Education in KSA for funding this research work through the project number IFP-KKU-2020/8.

References

- [1] K. Pach-Zawada, E. Golis, P. Pawlik, K. Kotynia, R. Miedziński, J. Filipecki, *Physica B: Condensed Matter* **562**, 36 (2019).
- [2] A. Jha, S. Shen, M. Naftaly, *Phys. Rev.* **62**, 6215 (2000).
- [3] M. El-Okri, M. Ibrahim, M Farouk, *Journal of Physics & Chemistry of Solids* **69**, 2564 (2008).
- [4] El S. Yousef, M. M. Elokr, Y. M. Aboudeif, *Chalcogenide Letters* **12**, 597 (2015).
- [5] S. D. Pandey, K. Samanta, J. Singh, N. D. Sharma, A. K. Bandyopadhyay, *Journal of Applied Physics* **116**, 133504 (2014).
- [6] K.A. Bashar, G. Lakshminarayana, S. O. Baki, Al-B. F. A. Mohammed, U. Caldino, A. N. Meza-Rocha, Vijay Singh, I. V. Kityk, M. A. Mahdi, *Opt. Mater.* **88**, 558 (2019).
- [7] N. Wantana, E. Kaewnuam, B. Damdee, S. Kaewjaeng, S. Kothan, H. J. Kim, J. Kaewkhao, *J. Lumin.* **194**, 75 (2018).
- [8] B. J. Riley, H. S. Park, J. H. Choi, K. R. Lee, W. L. Ebert, N. L. Canfield, *Journal of Nuclear Materials* **539**, 152313 (2020).
- [9] R. Kaur, A. Khanna, *Journal of Luminescence* **225**, 117375 (2020).
- [10] C. D. Peter, *J. Appl. Phys.* **111**, 07A721 (2012).
- [11] J. Animesh, R. Billy, J. Gin, T. F. Toney, J. Purushottam, X. Jiang, L. Joris, *Mater. Sci.* **57**, 1426 (2012).
- [12] L. Harris, D. Ottaway, P. J. Veitch, *Appl Phys B* **106**, 429 (2012).
- [13] M. N. Deeter, G. W. Day, A. H. Rose, in M. J. Weber (ed.) *CRC Handbook of Laser Science and Technology, Supplement 2: Optical Materials* (CRC Press, Boca Raton, 1994), Sect. 9
- [14] K. J. Prashant, Y. Xiao, *Nano letter* **9**(41644), (2009).
- [15] Q. Chen, *Journal of Alloys and Compounds* **828**, 154448 (2020).
- [16] Q. Chen, K. Su, *J. Non-Cryst. Solids* **495**, 75 (2018).
- [17] H. Mikhail, I. Mekawy, *Czech J Phys* **28**, 216 (1978).
- [18] E. P. Golis, A. Ingram, *Journal of Physics, Conference Series* **790**12003, (2007).
- [19] H. Akamatsu, K. Fujita, Y. Nakatsuka, S. Murai, K. Tanaka, *Optical Materials* **35**, 1997 (2013).
- [20] J. Qiu, J.B. Qiu, H. Higuchi, Y. Kawamoto, K. Hirao, *Journal of applied physics* **80**, 5297 (1996).
- [21] A. M. Emara, M. M. Alqahtani, Y. M. Abou Deif, El Sayed Yousef, *Chalcogenide Letters* **14**, No. 9, 405, (2017).
- [22] H. Fares, I. Jlassi, H. Elhouichet, M. Férid, *Journal of Non-Crystalline Solids* **396–397**,

- 1 (2014).
- [23] G. Upender, V. G. Sathe, V. C. Mouli, *Physica B: Condensed Matter* **405**, 1269 (2010).
- [24] W. C. Wang, W. J. Zhang, L. X. Li, Y. Liu, D. D. Chen, Q. Qian, Q. Y. Zhang, *Optical Materials Express* **6**, 2095 (2016).
- [25] El S. Yousef, H. H. Hegazy, M. M. Elokr, Y. M. Aboudeif, *Chalcogenide Letters* **12**, 653 (2015).
- [26] V. Kamalaker, G. Upender, Ch. Ramesh, V. Chandra Mouli, *Spectrochimica Acta Part A* **89**, 149 (2012).
- [27] Y. M. Aboudeif, M. M. Alqahtani, A. M. Emar, H. Algarni, El S. Yousef, *Chalcogenide Letters* **15**, 219 (2018).
- [28] J. Lin, W. Huang, Z. Sun, C.S. Ray, D. E. Day, *Journal of Non-Crystalline Solids* **336**, 189 (2004).